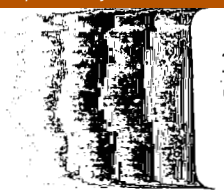

NASA CONTRACTOR REPORT

CLOUD MOTION IN RELATION TO THE AMBIENT WIND FIELD

Henry E. Fuelberg and James R. Scoggins

Prepared by
TEXAS A&M UNIVERSITY
College Station, Texas 77843
for George C. Marshall Space Flight Center

NATIONAL AERONAUTICS AND SPACE ADMINISTRATION • WASHINGTON, D. C. • MAY 1975

1. REPORT NO.	2. GOVERNMENT ACCESSION NO.	3. RECIPIENT'S CATALOG NO.
NASA CR-2557		

4. TITLE AND SUBTITLE	5. REPORT DATE
Cloud Motion in Relation to the Ambient Wind Field	MAY 1975
	6. PERFORMING ORGANIZATION CODE M144
7. AUTHOR(S) Henry E. Fuelberg and James R. Scoggins	8. PERFORMING ORGANIZATION REPORT #
9. PERFORMING ORGANIZATION NAME AND ADDRESS Center for Applied Geosciences, Texas A&M University, College Station, Texas 77843	10. WORK UNIT NO.
	11. CONTRACT OR GRANT NO. NAS8-26751
12. SPONSORING AGENCY NAME AND ADDRESS National Aeronautics and Space Administration, Washington, D. C. 20546	13. TYPE OF REPORT & PERIOD COVERED Contractor Report
	14. SPONSORING AGENCY CODE

15. SUPPLEMENTARY NOTES This report is based on work performed under Contract NAS8-26751 and is published to describe the trajectories of clouds computed from a mathematical model and compared with radar data from the AVE II Experiment. This work was conducted under the direction of Robert Turner, MSFC, for the Office of Applications, NASA Hq.

16. ABSTRACT

Trajectories of convective clouds were computed from a mathematical model and compared with trajectories observed by radar. The ambient wind field was determined from the AVE IIP data. The model includes gradient, coriolis, drag, lift, and lateral forces. The results show that rotational effects may account for large differences between the computed and observed trajectories and that convective clouds may move 10 to 20 degrees to the right or left of the average wind vector and at speeds 5 to 10 m/sec faster or slower than the average ambient wind speed.

17. KEY WORDS	18. DISTRIBUTION STATEMENT
atmospheric sounding clouds radar models	UNCLASSIFIED – UNLIMITED CAT 47

19. SECURITY CLASSIF. (of this report)	20. SECURITY CLASSIF. (of this page)	21. NO. OF PAGES	22. PRICE
UNCLASSIFIED	UNCLASSIFIED	36	$3.75

FOREWORD

This report is one of several to be published from research conducted under NASA Contract NAS8-26751 entitled "Cloud Motion in Relation to the Ambient Wind Field". This effort is sponsored by the NASA Office of Applications under the direction of Marshall Space Flight Center's Aerospace Environment Division. The results presented in this report represent only a portion of the total research effort. Other reports will be published as the research progresses. Data used in the report were taken from the AVE II Experiment conducted during a 24-hour period beginning at 1200 GMT on May 11, 1974, and ending at 1200 GMT on May 12, 1974.

TABLE OF CONTENTS

LIST OF TABLES

LIST OF FIGURES

CLOUD MOTION IN RELATION TO THE AMBIENT WIND FIELD

by

Henry E. Fuelberg[1]

and

James R. Scoggins[2]

Center for Applied Geosciences
Texas A&M University

I. INTRODUCTION AND BACKGROUND

The second Atmospheric Variability (Pilot) Experiment (AVE IIP) has provided data from which observed cloud motions can be compared with the known wind field obtained from upper-air soundings. Cloud motions may be determined from successive satellite or radar pictures. Radar is especially useful in tracking convective clouds because the center of the cloud can be determined readily by varying the attenuation or elevation angle of the radar set, and because the cloud systems can be continuously monitored. Satellites provide a means of tracking clouds which are not usually detected by radar, but it is sometimes difficult to find distinguishable features of non-convective clouds which can be tracked. Initial results of research on the movements of convective clouds indicated by radar in relation to wind obtained from rawinsonde data are presented in this report.

The motion of convective clouds in relation to the ambient wind field has received considerable attention, and for many years meteorologists believed that these clouds moved very nearly with the wind field in which they were imbedded. Humphreys (1940) states, "The velocity of the thunderstorm is nearly the velocity

---

[1]Research Assistant, Center for Applied Geosciences, Texas A&M University

[2]Professor of Meteorology and Director, Center for Applied Geosciences, Texas A&M University

of the atmosphere in which the bulk of the cloud is located." Studies have been conducted to show the relation between the movement of radar echoes and the winds at some particular level or average of several levels. Byers and Braham (1949), Ostergoard (1948), and Hiser and Bigler (1953) found high correlations between storm movements and average winds within the cloud-bearing layers which supported the earlier findings of Humphreys. Brooks (1946) showed that small radar echoes move with the wind at the 5,000-ft level and that larger ones move with the winds of the 11,000-ft level. Ligda and Mayhew (1954) found close correlations between the geostrophic wind computed from 700-mb analyses and the movement of precipitation echoes associated with the polar front.

Further research has indicated that much lower correlations are found between observed winds and the movements of large, severe thunderstorms. Newton and Katz (1958) studied the movement of large convective rainstorms relative to the wind at 700 mb and found that these storms track from 10° to 25° to the right of the wind at 700 mb. The deviation was thought to be due to continuing development on the right side of the storm with concurrent dissipation on the left. Newton and Newton (1959) suggested that a vertical gradient of nonhydrostatic pressure is generated at the cloud boundaries which enhances new cloud growth in a favored region and produces deviation. Newton and Frankhauser (1964) found that in a veering wind field the largest thunderstorms deviated as much as 60° to the right of the average wind, while the smaller storms moved as much as 40° to the left. They related the motions of the storms to the available water vapor supply and to storm size. Fujita and Grandoso (1968) developed a numerical model of a thunderstorm that considered dynamical forces, and concluded that storms deviate to the left of the average wind unless they rotate slowly and cyclonically. They found that the maximum deviation, either to the left or right, occurs when a thunderstorm rotates with a tangential speed of only a few meters per second. Costen (1972) has shown that a rotating severe local storm that

is tilted from the vertical may drift with respect to the ambient fluid because the buoyancy force on the tilted updraft has a component transverse to the axis of the storm.

Although a great deal of research effort has been spent in the study of storm trajectories, much work remains to be done. The AVE Project hopes to contribute to a better understanding of storm motions so that meaningful winds may be inferred from these motions.

II. CORRELATION OF ECHO MOVEMENTS WITH WIND VELOCITY

A. Procedure

Echo movements at Monette, Missouri, have been related to the ambient wind field. Monette is the site of a rawinsonde station and a WSR-57 radar station operated by the National Weather Service and is centrally located within the AVE IIP rawinsonde network. Precipitation activity near Monette was associated with a cold front which passed near 1800 GMT on May 11 and consisted of near solid lines of echoes as well as discrete cells. Time-lapse radar pictures taken at intervals of about 5 min were used in the study. The 16 mm films were projected onto sheets of paper from which the speed and direction of echo movement were computed. Echo centroids of discrete cells were estimated by ascribing a "best-fit" geometric simplification (rectangle, circle, or ellipse) to the echo contour and then tracked over a time period that averaged about 45 min. Echo diameters used in the study were average values obtained during the tracking period. An "equal area" simplification was used to obtain the diameters of non-circular storms. Echoes which merged or split during the tracking period were not considered, and an effort was made to include only clouds that were near the middle of their life cycles. The movements of individual components of echo lines were computed by tracking distinguishable features along the line.

Ambient wind conditions were obtained from rawinsonde soundings at Monette. The average wind in the 900-200-mb layer was obtained from the equation:

$$\vec{\bar{V}}_{9-2} = \frac{\vec{V}_{850} + \vec{V}_{700} + \vec{V}_{500} + \vec{V}_{300}}{4} \cdot \qquad (1)$$

This equation was used by Fankhauser (1964) who states that the resultant value can be considered representative of the winds in a cloud-bearing layer extending to 40,000 ft. Although the exact heights of all the echoes studied at Monette could not be determined, the average was below 40,000 ft. The average wind in the layer from

900-400 mb was computed using the equation:

$$\vec{V}_{9-4} = \frac{\vec{V}_{850} + \vec{V}_{700} + \vec{V}_{500}}{3} . \qquad (2)$$

The motions of echoes tracked within 90 min of a rawinsonde sounding were compared with winds obtained from that sounding. Since only echoes that were within 125 n mi of Monette and within 90 min of a rawinsonde sounding were considered, the determination of winds at the actual storm location was not made.

B. Results of Line Echo Studies

Rawinsonde wind profiles at Monette from 1200 GMT, 11 May to 1200 GMT, 12 May 1974 are shown in Fig. 1, and corresponding hodographs in Figs. 2-6. Table 1 indicates average winds from 900-400 mb, and 900-200 mb for the five time periods during which echoes were observed. No precipitation echoes were observed at Monette after approximately 0200 GMT.

Table 1. Observed Average Winds at Monette, Missouri from 1200 GMT, 11 May 1974, to 0000 GMT, 12 May 1974

Time (GMT)	Average Wind (900-400 mb) (deg - m/sec)	Average Wind (900-200 mb) (deg - m/sec)
1200	255 - 7.0	237 - 8.9
1500	275 - 7.2	248 - 8.5
1800	288 - 10.5	273 - 12.3
2100	295 - 12.7	283 - 13.6
0000	294 - 18.5	293 - 18.2

Portions of a well-defined line of echoes were observed at Monette during the period from 1030 GMT to 1630 GMT. Maximum tops of 38,000 ft were reported although the majority of echo tops were less than 30,000 ft. Surface reports indicated rain and rainshowers in the area although an isolated thundershower

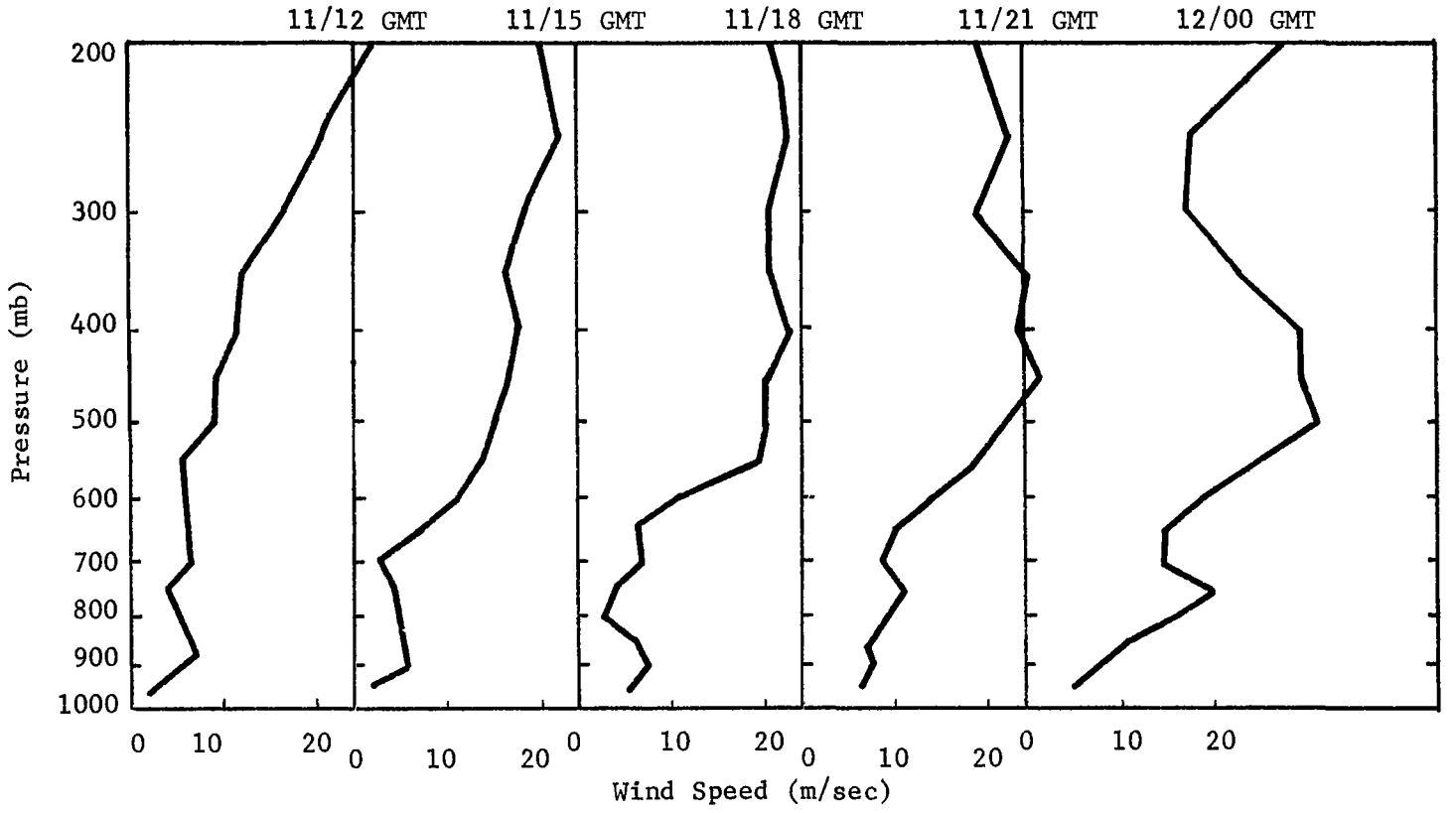

Fig. 1. Time series of wind speed at Monette, Missouri from 1200 GMT, 11 May 1974, to 0000 GMT, 12 May 1974.

may have escaped detection. The line as observed from Monette extended from 295° at 115 n mi to 35° at 125 n mi at 1200 GMT. The line continued northeastward but out of range of the Monette radar. The northeastern portion of the line was moving from 330° at 4.2 m/sec while individual elements in the area were moving from 243° at 15.4 m/sec. This area of the line was moving 75° to the right of the lower average direction (900-400 mb) and 93° to the right of the upper average direction (900-200 mb), while its speed was 2.8 m/sec slower than the lower average speed and 4.7 m/sec slower than the upper average speed. The southwestern portion of the line also moved from 330° but at 6.2 m/sec which is 2.0 m/sec closer to the average wind speed at either level. Individual elements in this area moved from 290° at 10.0 m/sec. Individual elements moved strongly to the left of the line movement in both areas, moved faster than either average wind speed, and faster than the line motion.

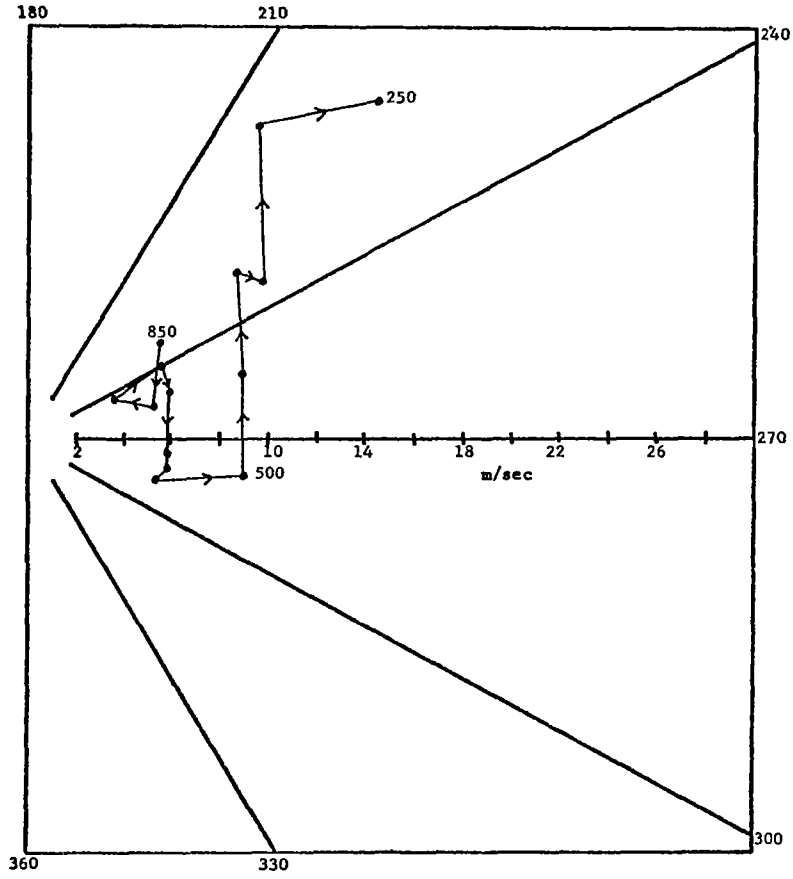

Fig. 2. Hodograph of winds at Monette, Missouri at 1200 GMT, 11 May 1974. Values are plotted at 50-mb intervals.

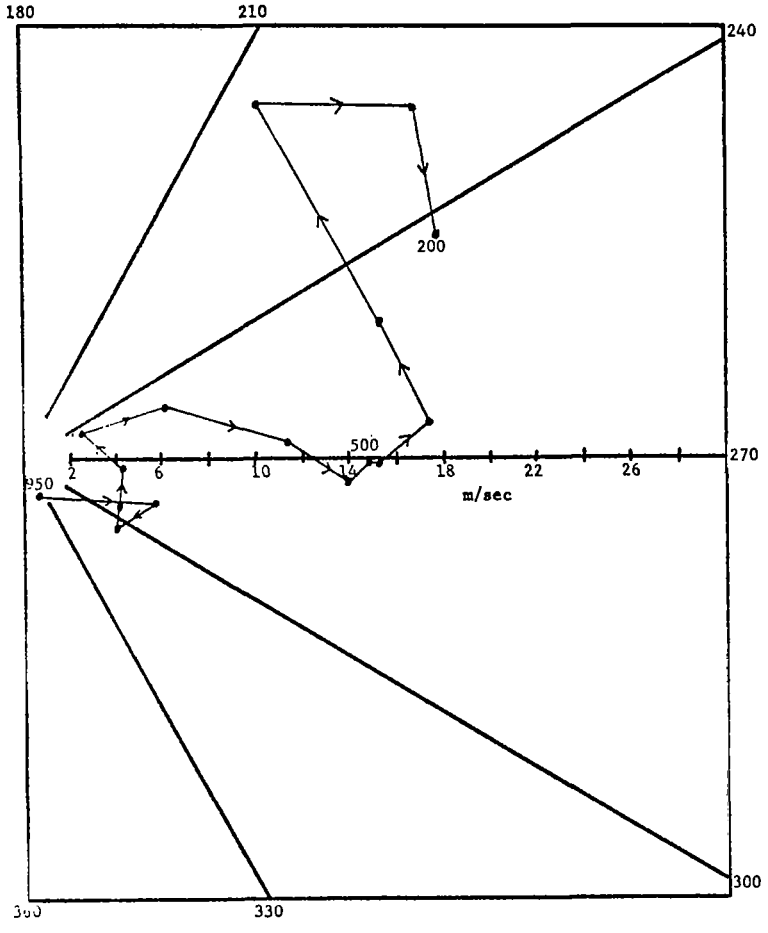

Fig. 3. Hodograph of winds at Monette, Missouri at 1500 GMT, 11 May 1974. Values are plotted at 50-mb intervals.

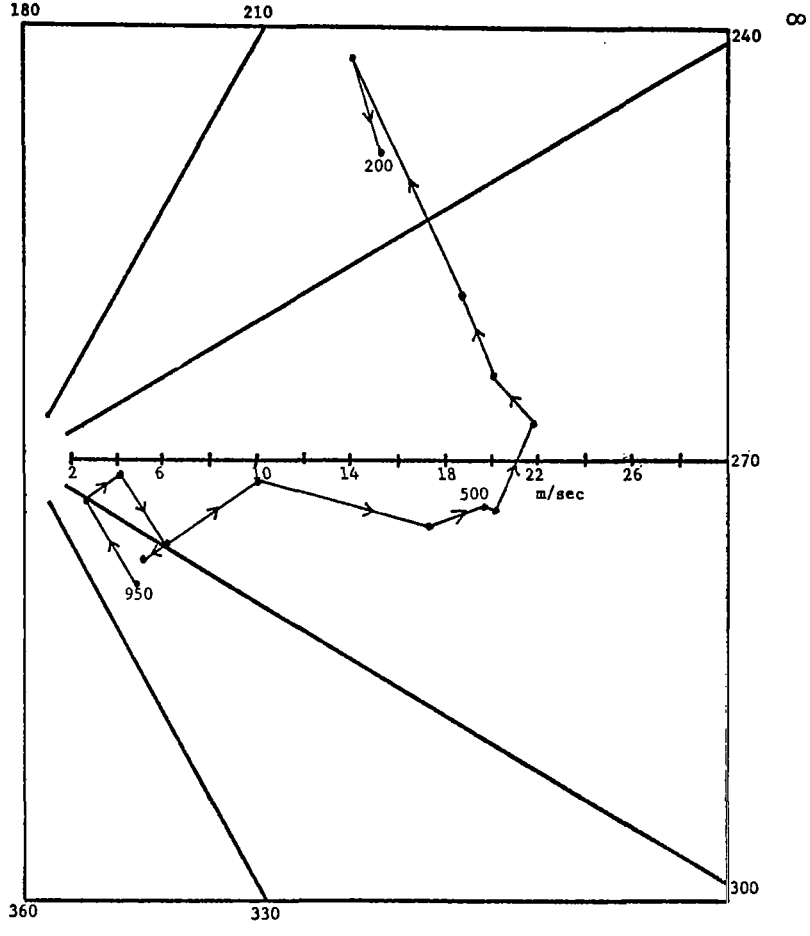

Fig. 4. Hodograph of winds at Monette, Missouri at 1800 GMT, 11 May 1974. Values are plotted at 50-mb intervals.

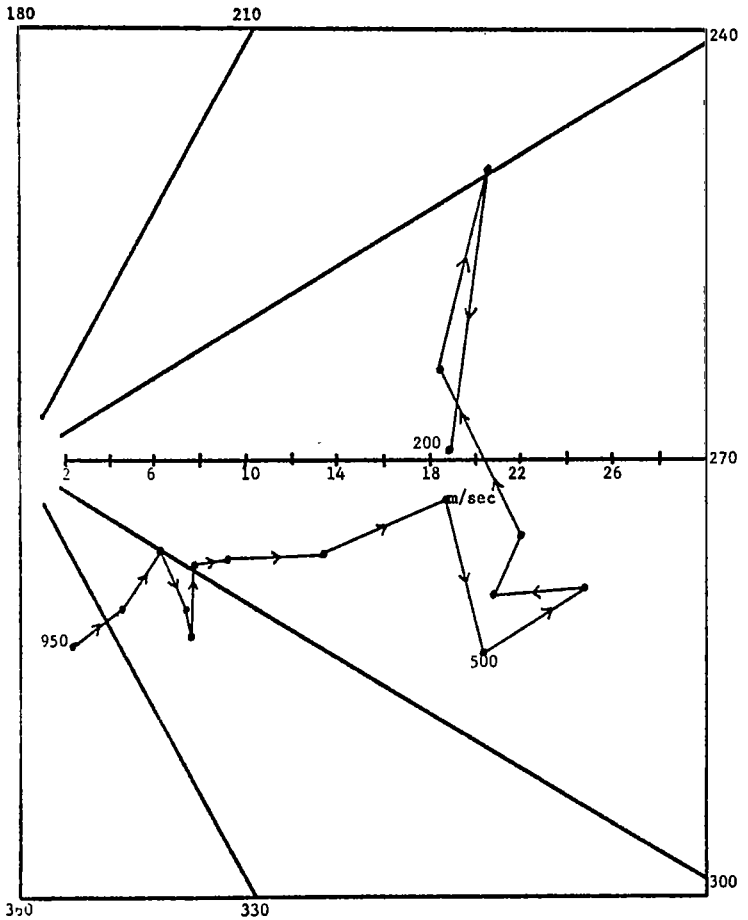

Fig. 5. Hodograph of winds at Monette Missouri at 2100 GMT, 11 May 1974. Values are plotted at 50-mb intervals.

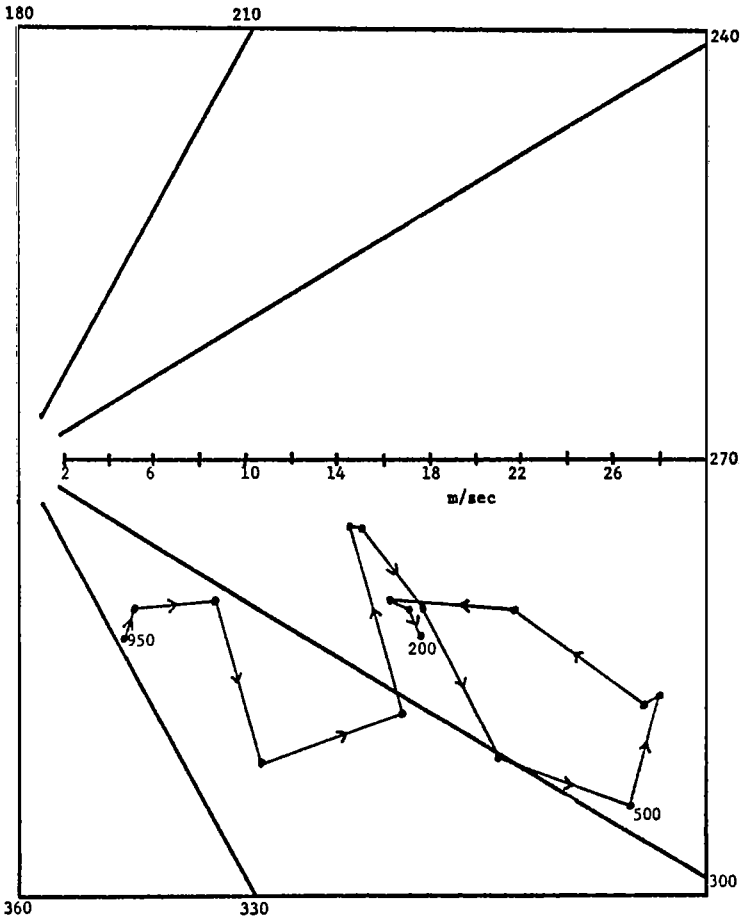

Fig. 6. Hodograph of winds at Monette, Missouri at 0000 GMT, 12 May 1974. Values are plotted at 50-mb intervals.

At 1500 GMT the segment of the line observed at Monette extended from 325° at 35 n mi to 20° at 125 n mi and then beyond radar range. The width of the line had decreased since 1200 GMT, and shortly after 1500 GMT the segment of the line observed at Monette dissipated into an area of scattered echoes. All portions of the line moved from 305° at 7.7 m/sec or 30° to the right of the lower average direction and 57° to the right of the upper average direction. Although the average wind direction of the lower layer changed from 255° at 1200 GMT to 275° at 1500 GMT, the direction of the line movement changed in the opposite sense, from 330° at 1200 GMT to 305° at 1500 GMT. Individual elements in the northeastern portion of the line moved from 225° at 16.5 m/sec while those in the southwestern portion moved from 265° at 17.1 m/sec. These changes in direction with time were also opposite the changes in the average wind direction, but individual elements continued to move well to the left of the line motion. The individual elements of the northeastern portion of the line tended to move to the left of the average directions at both time periods, while elements in the southwestern section tended to move strongly to the right of the average wind directions at 1200 GMT, but much less to the right at 1500 GMT. The speeds of cells in the northeastern portion changed little while speeds of cells in the southwestern segment increased approximately 7.0 m/sec; cells continued to move faster than the average winds and the line itself. Changes in the average wind speed at Monette were less than 0.5 m/sec in both layers.

Explanations for the observed cell and line movements with respect to each other, and with respect to the observed average wind, are not readily apparent. A major complication is that observed line and cell movements are due to growth and dissipation processes as well as advection. Constant-pressure maps on the synoptic scale do not reveal wind direction shears in the horizontal direction in the vicinity of Monette that would explain the observed motions. The presence of a jet stream to the north of the area suggests a more rapid movement of echoes in that area which was

observed at 1200 GMT but not at 1500 GMT. Figures 2-3 indicate only minor turning of the wind with height below 500 mb, but backing winds with height above 500 mb. Fankhauser (1964) observed squall lines in conditions of small turning of the wind with height, and concluded that new elements form on the upwind (SW) side of existing squall lines, move faster than the line as a whole, and eventually dissipate on the downwind (NE) side. Newton and Fankhauser (1964) observed similar results for storms occurring under conditions of strong winds aloft which veer with height. They observed that under these conditions, a movement of individual echoes to the left, nearly along, or to the right of the average wind may take place, depending on the size of the echo. Both of these papers and most other papers dealing with lines of echoes are concerned with severe convective activity, but this was not observed near Monette. These results indicate that motions generally associated with severe squall lines may be associated with lines of rainshowers and thundershowers. Further research will be necessary to confirm these findings, but if they are confirmed, changes will be required in current theories explaining the motions of lines of echoes.

C. Individual Echo Studies

Beginning at about 1300 GMT on May 11 and continuing until about 0200 GMT on May 12, numerous discrete echoes were tracked near Monette. Tops of the clouds averaged approximately 30,000 ft, although near the end of the period some isolated tops extended to near 38,000 ft. Average winds in the layer from 900-400-mb taken from the rawinsonde sounding closest in time were used for comparison with echo movements. The tracks of the echoes (each determined over a period of about 45 minutes) considered are shown in Fig. 7. Table 1 indicates that the average wind direction in the 900-400-mb layer at Monette changed from 275° at 7.2 m/sec to 294° at 18.5 m/sec between 1500 GMT and 0000 GMT. Figures 3-6 indicate a vertical wind field at Monette which generally backs with height.

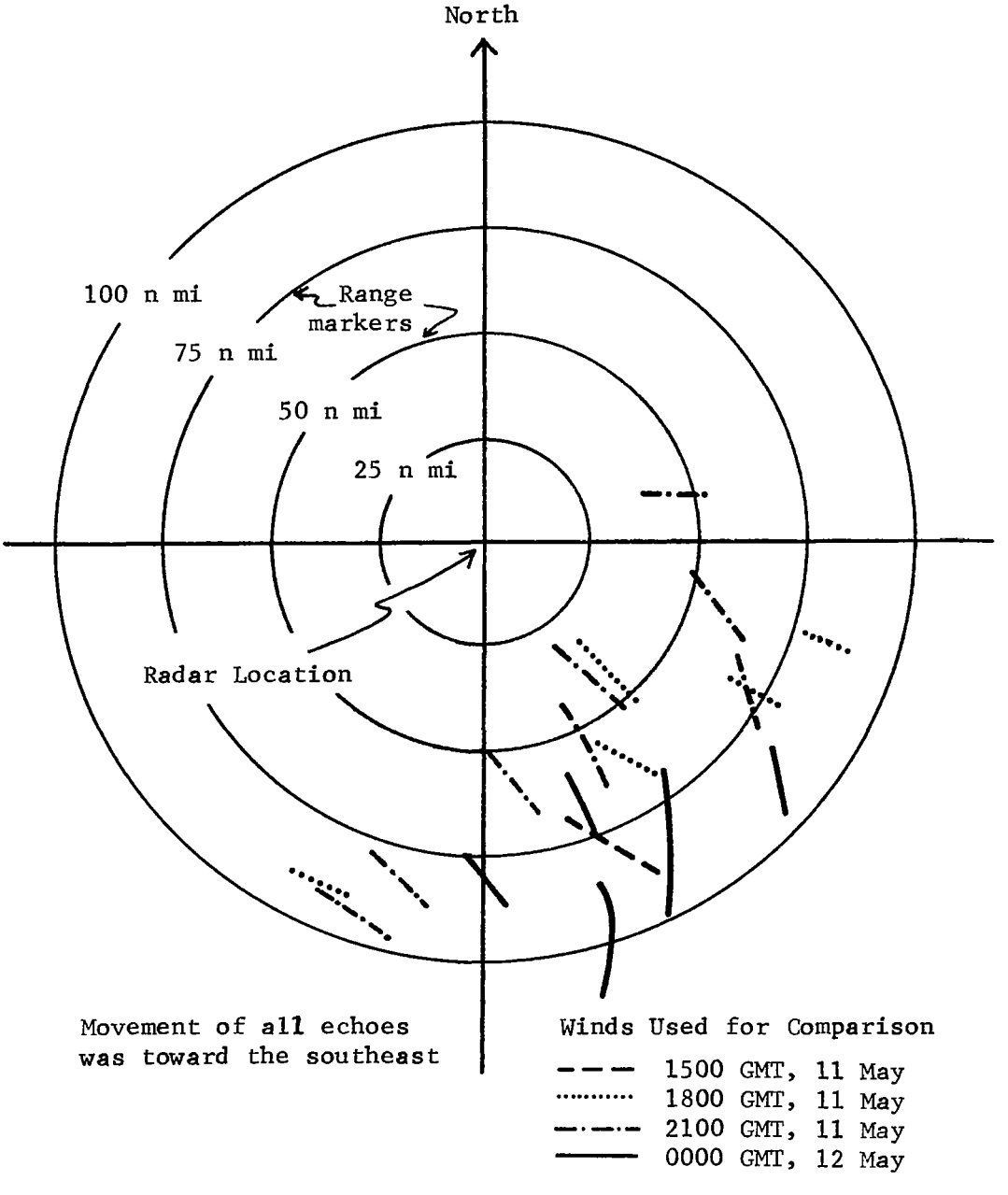

Fig. 7. Tracks of individual echoes observed near Monette. The time period was from 1300 GMT on 11 May 1974 to 0200 GMT on 12 May 1974.

Figure 8 indicates that most of the echoes moved to the right of the average wind in the 900-400-mb layer while Fig. 9 shows that the clouds moved slower than the average wind in the same layer. Correlations between echo velocity and wind velocity at individual levels were made, and wind velocity at 700-mb produced the best results (Figs. 10 and 11). This finding is similar to those stated by Ligda and Mayhew (1954) and Newton and Katz (1958). Figures 12 and 13 indicate that the deviations of echo movement from average wind conditions in the layer from 900-400-mb are related to storm diameter. Larger echoes moved slower and more to the right of the average wind than did smaller echoes. Similar results were obtained by Newton and Fankhauser (1964) in the case of severe storms which occurred in a wind field that veered strongly with height, but Fankhauser (1964) found that severe storms occurring in a field that exhibited little turning with height moved very nearly with the average wind velocity. As a check on the Monette results, the average wind velocity at the site of the echo was computed and compared with the average wind at Monette for several cases. Only slight differences in the winds were found; this was expected since the echoes being studied were generally within 100 n mi of Monette. The motions usually attributed to severe storms in a veering wind environment appear, in this case, to characterize rainshowers and thundershowers occurring in a different wind regime. Further research will be necessary to confirm and explain these results.

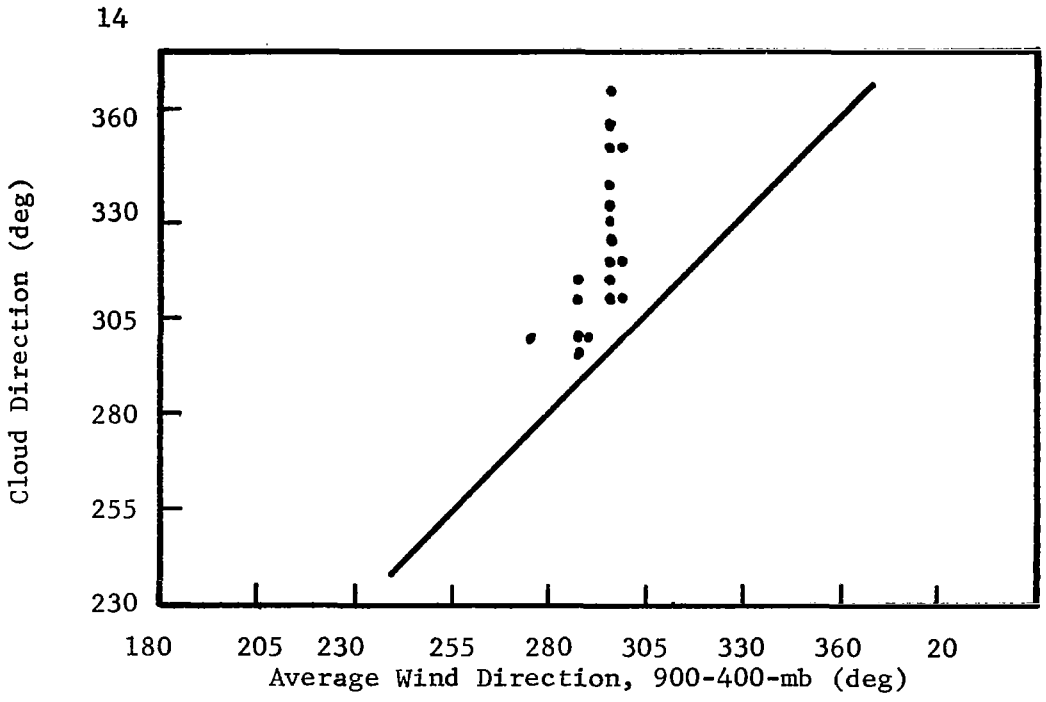

Fig. 8. Cloud direction versus average wind direction in the 900-400-mb layer.

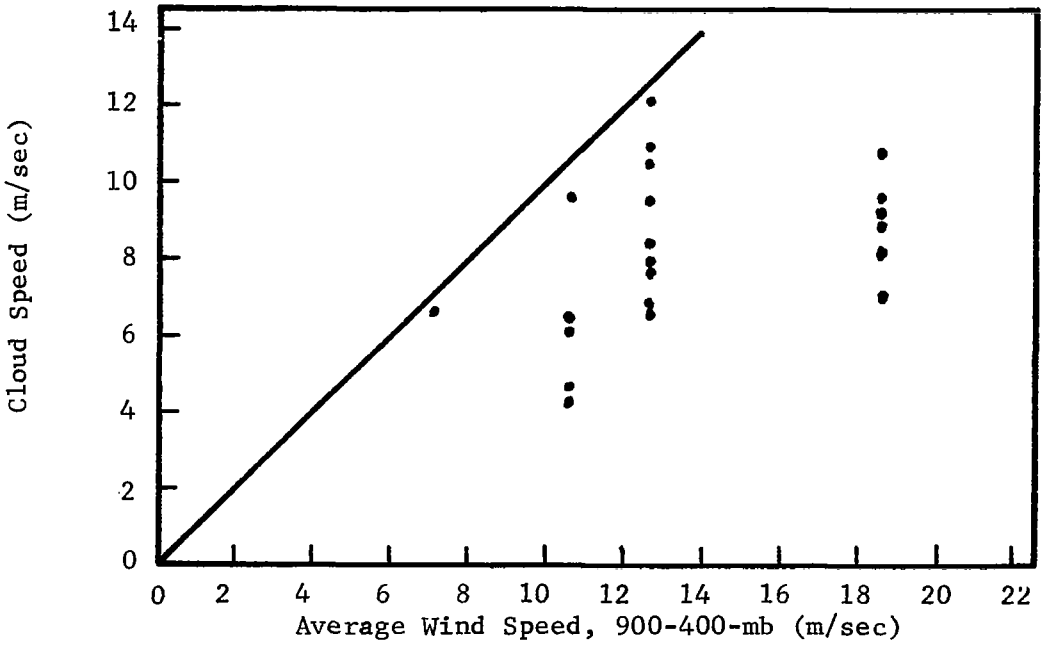

Fig. 9. Cloud speed versus average wind speed in the 900-400-mb layer.

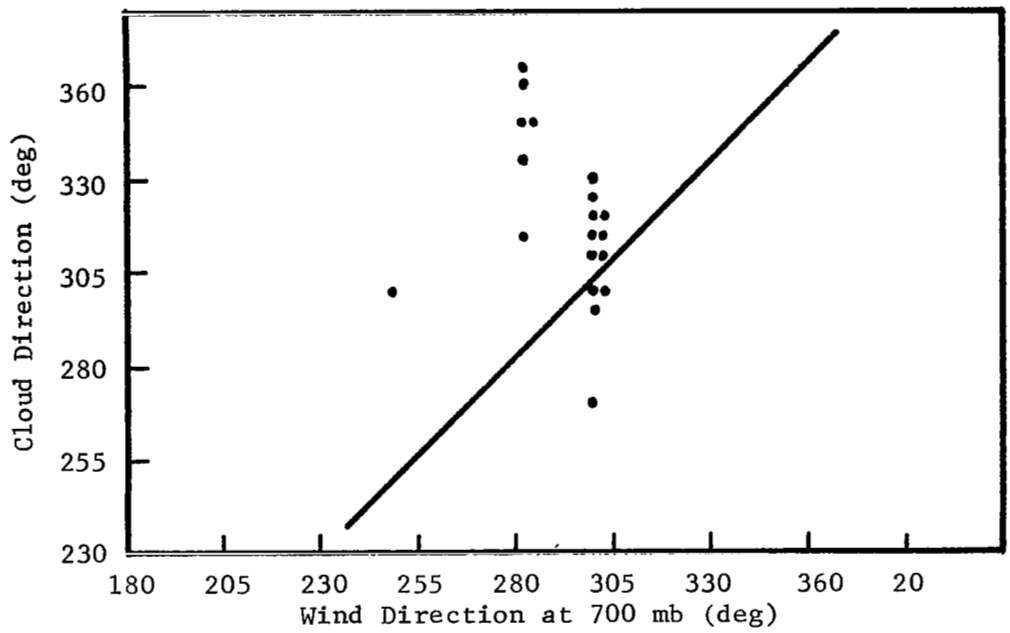

Fig. 10. Cloud direction versus wind direction at 700-mb.

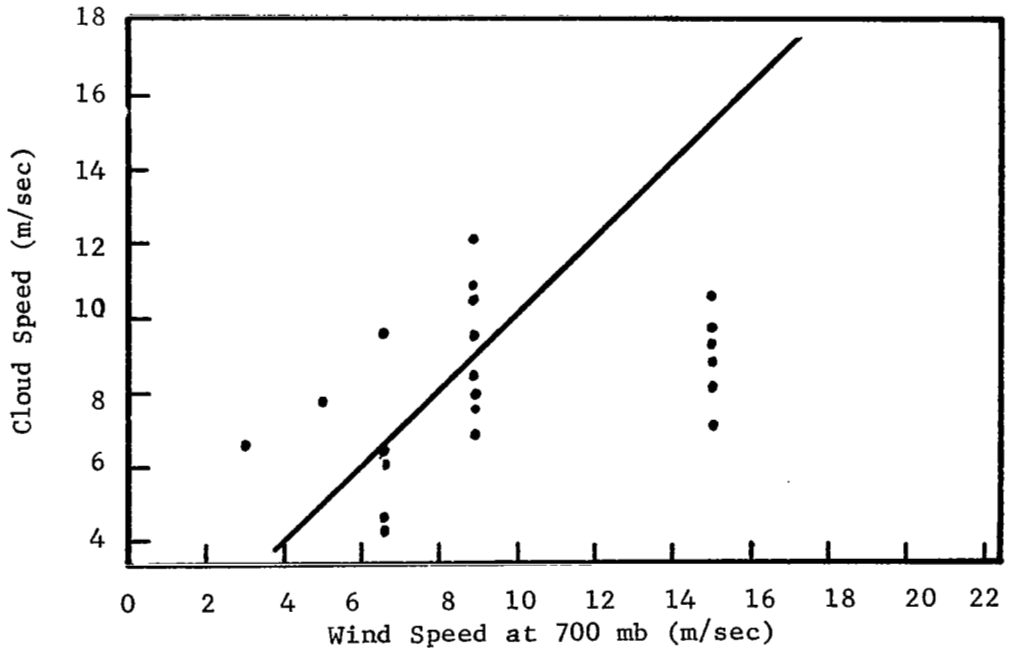

Fig. 11. Cloud speed versus wind speed at 700-mb.

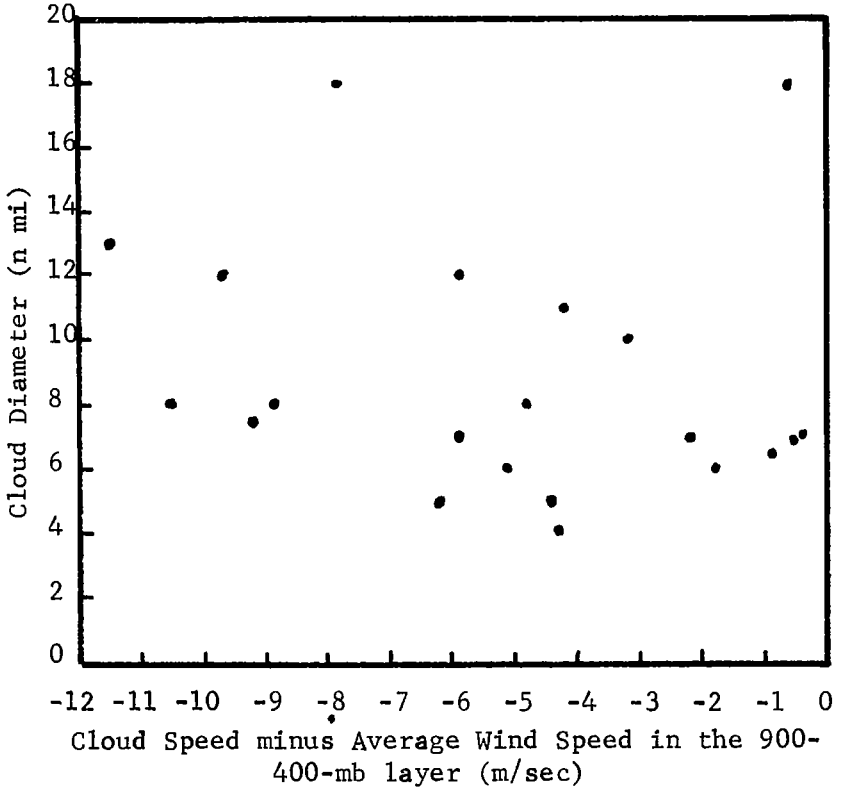

Fig. 12. Cloud diameter versus deviation of cloud speed from average wind speed in the 900-400-mb layer.

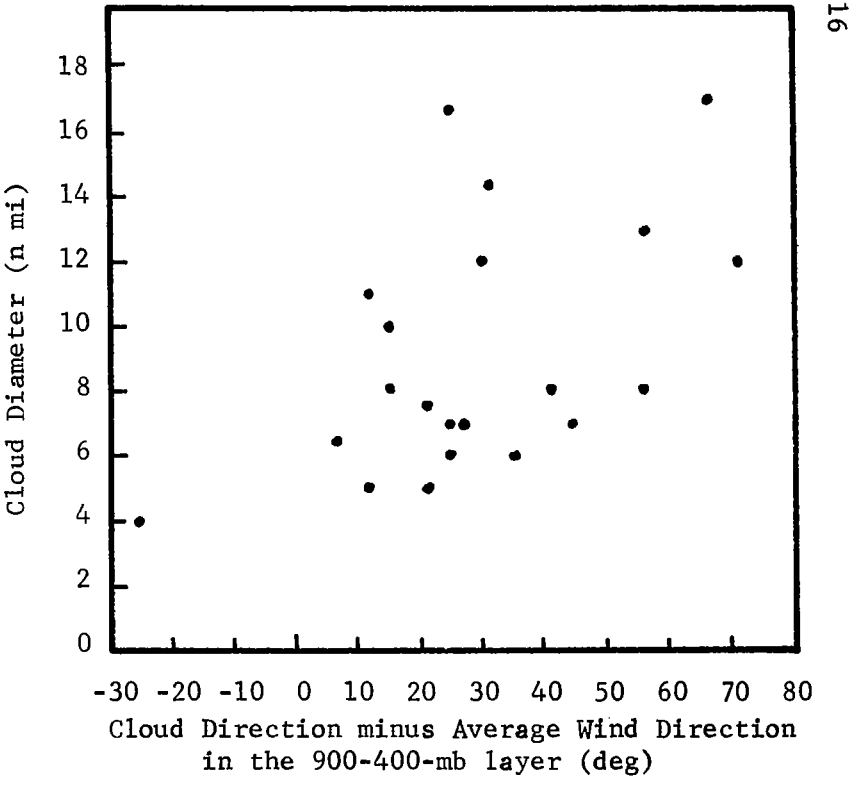

Fig. 13. Cloud diameter versus deviation of cloud direction from average wind direction in the 900-400-mb layer.

III. A NUMERICAL CLOUD MODEL

Veazey (1968) investigated a simple numerical cloud model based on earlier work by Fujita and Grandoso (1968). The model described in this section is based on the work by Veazey. The model considers clouds to be solid cylinders of rotation that can revolve either cyclonically or anticyclonically about a central vertical axis. Vertical motion, entrainment, the penetrability of the cylinder, and mixing are neglected. The forces per unit cloud mass that were used in the model are:

(1) Gradient force,

$$\vec{F}_G = -f\vec{W} \times \vec{k}, \tag{3}$$

where $\vec{W}$ is the geostrophic wind vector, $\vec{k}$ is the unit vector oriented toward the local zenith, and f is the coriolis parameter.

(2) Coriolis force,

$$\vec{F}_C = f\vec{S} \times \vec{k}, \tag{4}$$

where $\vec{S}$ is cloud velocity.

(3) Drag force,

$$\vec{F}_D = \frac{2}{\pi D} C_D \vec{U} |\vec{U}|, \tag{5}$$

where $\vec{U}$ is the wind vector relative to the moving cloud, $(\vec{W}-\vec{S})$, C_D is the drag coefficient, and D is the diameter of the cloud.

(4) Kutta-Joukowski force (lift force)

$$\vec{F}_L = \frac{4}{D} V_\theta |\vec{U}| (\vec{r} \times \vec{k}), \tag{6}$$

where V_θ is the tangential speed of the rotating cylinder (cyclonically positive), and $\vec{r}$ is a unit vector in the direction of $\vec{U}$.

(5) Lateral shear force,

$$\vec{F}_S = \overline{U} \frac{\partial W}{\partial N} (\vec{r} \times \vec{k}), \tag{7}$$

where $\partial W/\partial N$ is the lateral shear and $\overline{U}$ is the average speed of the environmental flow relative to the moving cloud. This force has been described by Darkow (1968).

The resultant force acting on each level of the cloud is given by:

$$F_r = \left[\left(-fU + \frac{4}{D} V_\theta U + \overline{U} \frac{\partial W}{\partial N}\right)^2 + \left(\frac{2}{\pi D} C_D U^2\right)^2\right]^{\frac{1}{2}} \qquad (8)$$

while the azimuth angle of the resultant force, ϕ, measured from $\vec{U}$ is given by:

$$\phi = \text{TAN}^{-1}\left[\frac{-fU + \frac{4}{D} V_\theta U + \overline{U} \frac{\partial W}{\partial N}}{\frac{2}{\pi D} C_D U^2}\right] . \qquad (9)$$

Input for the model consisted of assumed values of C_D and V_θ, measured values of latitude and storm diameter (obtained from radar data), and measured values of actual wind and lateral shear at 850, 700, 500, and 300 mb. The wind values were weighted so that the sum of the forces at each level had an equal influence on cloud motion because of the unit mass consideration used in the force equations.

Clouds were assumed to initially move at the velocity of the observed 700-mb wind. The resultant forces were obtained using Eqs. (8) and (9). It was assumed that the entire cloud mass moved in the direction of the resultant force obtained by summing over all four levels. This required that each of the resultant forces computed at the four levels be brought to the center of the cloud and added vectorially. The cloud velocity resulting from this computation is called the "inertia" velocity by Fujita and Grandoso (1968). The forecast value of cloud velocity ($\vec{V}_1$) was then obtained from:

$$\vec{V}_1 = \vec{V}_0 + \vec{F}_r \Delta t, \qquad (10)$$

where $\vec{V}_0$ is the previous velocity, $\vec{F}_r$ is the resultant force per unit mass, and Δt is the time interval between computations. A value of 8 min was used for Δt. The cloud trajectory over the time interval was considered to be a straight line so that

$$\vec{V}_T = \frac{\vec{V}_n + \vec{V}_{n-1}}{2} \qquad (11)$$

where $\vec{V}_T$ is the average cloud velocity over the time period Δt, and $\vec{V}_n$ and $\vec{V}_{n-1}$ are velocities at the beginning and end of the time interval, respectively. The distance traveled by the cloud (ΔL) is then given by:

$$\Delta L = \left| \vec{V}_T \right| \Delta t \ . \qquad (12)$$

The forecast values become the initial values for the next time step. Computations were performed over a period of 80 min.

IV. RESULTS

Veazey (1968) tested this model (with a few minor modifications) on two severe storms each containing a confirmed tornado. Values of diameter, drag coefficient, and storm rotation were varied over a range of possibilities. He found that the model was best suited for forecasting the trajectory of an echo whose diameter is determined when the radar gain is a maximum and with the antenna at 0° elevation. Although none of his computed storm tracks matched exactly the tracks of real storms, many of the computed tracks were more accurate than a forecast based on average winds would have been. Fujita and Grandoso (1968) investigated a much more sophisticated version of this model and were able to successfully simulate a thunderstorm couplet formed by an echo split.

Two examples are presented here to show the results of the model on observed storms. The first example involves a thunderstorm observed by radar at Cincinnati, Ohio between 2144-2338 GMT on May 11. The average distance of the storm from the station was 90 n mi, the maximum top of the storm during the period was approximately 38,000 ft, and the average diameter was 12.5 n mi. The storm moved toward 35° at 18.0 m/sec while the average wind velocity in the layer from 900-200 mb using Eq. (1) was toward 42° at 22.9 m/sec. Table 2 gives the observed wind data that were used as input for this storm.

Table 2. Wind Data Used as Input for the Cincinnati Echo Observed between 2144-2338 GMT, May 11, 1974.

Level (mb)	Wind Velocity (deg - m/sec)	Lateral Shear (sec^{-1})
850	33.0 - 18.1	-2.7×10^{-5}
700	33.0 - 24.9	-2.3×10^{-5}
500	50.0 - 21.9	-3.6×10^{-5}
300	47.0 - 27.6	-1.9×10^{-5}

Figure 14 shows tha actual storm trajectory, the trajectory based on movement at the computed average wind velocity, and three trajectories obtained from the model for tangential velocities of 1.0, 2.0, and 5.0 m/sec. Computed model velocities at the end of each 8-min time step also are given. The same information for tangential velocities of 0.0, -2.0, and -5.0 m/sec is given in Fig. 15. Since the actual value of the drag coefficient is unknown, a drag coefficient of 1.0 was used in these examples as was done by Fujita and Grandoso (1968). The values obtained using a rotation rate of 0.0, 1.0, and 2.0 are especially good when compared to the actual storm trajectory. One must remember that the initial storm velocity was the 700-mb wind velocity. The storm speeds that are listed show fluctuations at several values of tangential velocity; these were also observed by Veazey who found that their amplitudes were proportional to the magnitude of tangential velocity, but were also functions of the environmental wind speed and vertical shear. These oscillations affect the resulting trajectory somewhat, and are undesirable.

The vertically-weighted sums of the various forces up to 300 mb are given in Table 3 for the end of the 80-min period and for various rotation rates. The lift force is the predominate force for all cases except the non-rotating case. The magnitude of the forces increases as the tangential velocity increases and causes a larger relative velocity.

The second example of results from the model involves a series of four rainshowers observed near Cincinnati, Ohio between 1200-1314 GMT on May 11. The average distance of the echoes from Cincinatti was 75 n mi, the tops of the showers were estimated at 20,000 ft, and their average diameter was 9.0 n mi. The showers moved toward 30° at 18.0 m/sec while the average wind velocity in the layer from 900-400-mb computed using Eq. (2) was toward 35° at 14.2 m/sec. The observed wind data used as input into the model is given in Table 4. While the motion of these echoes did not differ greatly from that of the average wind, the example is presented to show

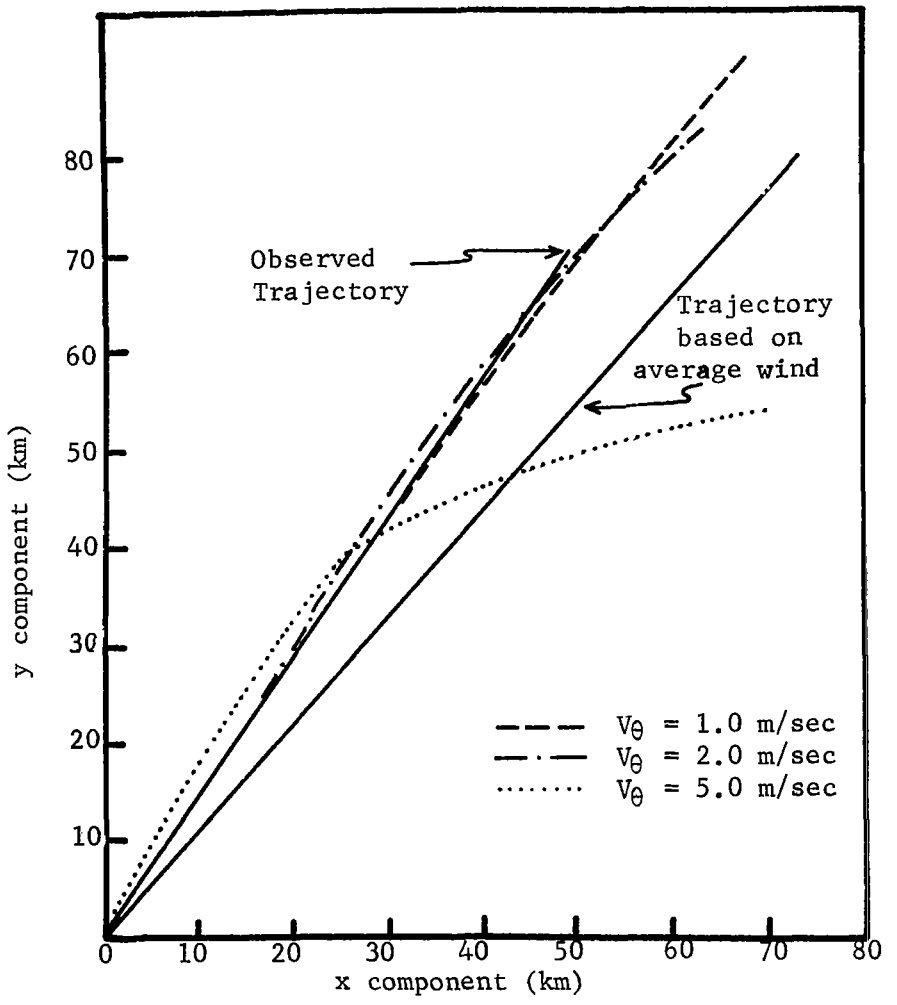

Computed Cloud Speeds (m/sec)

Time (min)	Assumed Tangential Velocity (m/sec)		
	V_θ =1.00	V_θ =2.00	V_θ =5.00
8	24.69	24.52	24.01
16	24,30	23.77	21.99
24	23.98	23.05	19.62
32	23.71	22.38	17.26
40	23.48	21.76	15.51
48	23.29	21.22	15.06
56	23.14	20.75	16.25
64	23.01	20.38	18.76
72	22.91	20.11	21.97
80	22.84	19.93	25.35

Fig. 14. Observed and computed trajectories at rotation rates of 1.0, 2.0, and 5.0 m/sec for the Cincinnati echo observed between 2144-2338 GMT. (The initial cloud velocity was assumed to be toward 33° at 24.9 m/sec, the echo diameter was 12.5 n mi, and the drag coefficient was 1.0. Computed cloud speeds are given to the right of the figure.)

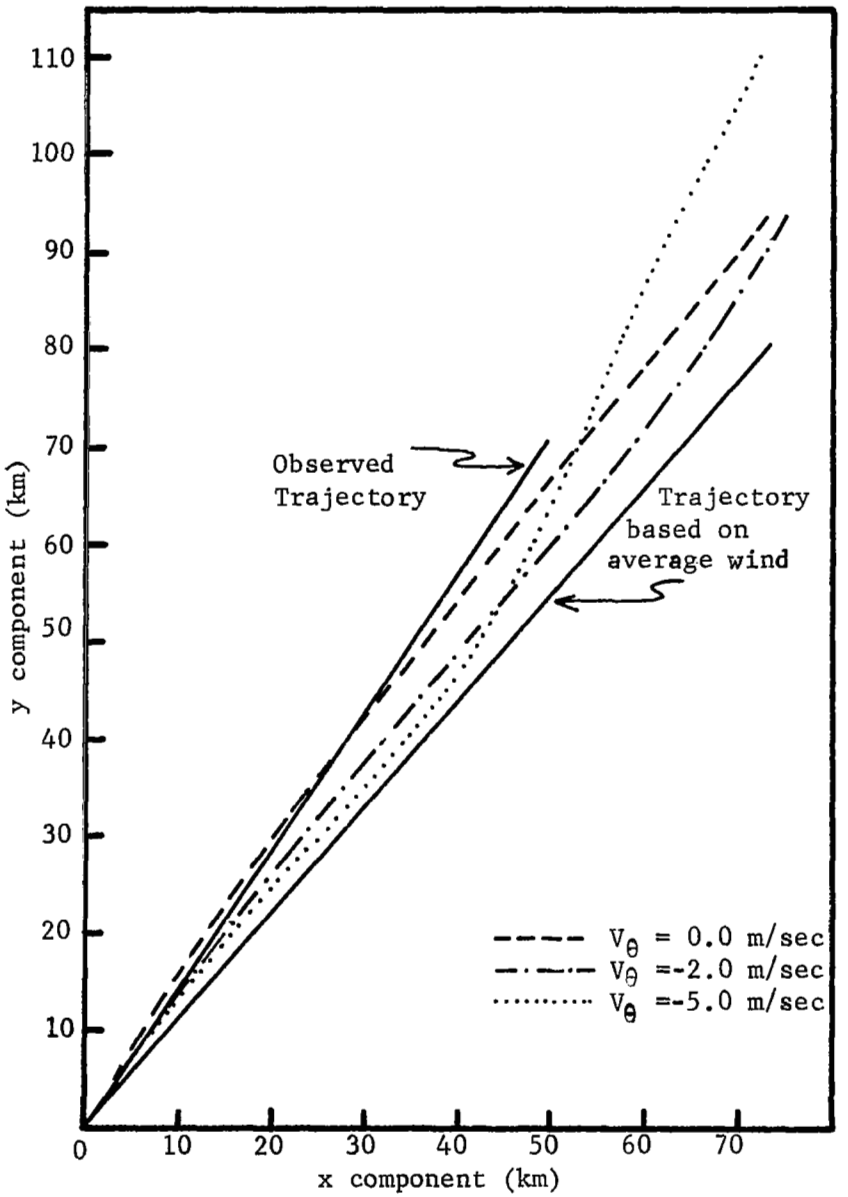

Computed Cloud Speeds (m/sec)

Time (min)	Assumed Tangential Velocity (m/sec)		
	V_θ =0.00	V_θ=-2.00	V_θ=-5.00
8	24.86	25.21	25.73
16	24.81	25.73	26.76
24	24.80	26.02	26.19
32	24.81	25.96	24.38
40	24.85	25.42	22.76
48	24.91	24.62	22.75
56	24.98	24.07	25.14
64	25.07	23.97	29.54
72	25.17	24.33	34.81
80	25.30	25.12	39.87

Fig. 15. Observed and computed trajectories at rotation rates of 0.0, -2.0, and -5.0 m/sec for the Cincinnati echo observed between 2144-2338 GMT. (The initial cloud velocity was assumed to be toward 33° at 24.9 m/sec, the echo diameter was 12.5 n mi, and the drag coefficient was 1.0. Computed cloud speeds are given to the right of the figure.)

Table 3. Vertically-Weighted Sums of the Forces* Considered for the Cincinnati Echo Observed between 2144-2338 GMT. The forces at 850, 700, 500, and 300 mb are weighted to give equal influence at each level and apply at the end of the period.

V_θ (sec^{-1})	F_G+F_C (m/sec^2)	F_D (m/sec^2)	F_L (m/sec^2)	F_S (m/sec^2)
-5.0	-0.0012	0.0052	-0.0118	-0.0003
-2.0	-0.0005	0.0009	-0.0021	-0.0001
0.0	-0.0004	0.0003	0.0000	-0.0001
1.0	-0.0004	0.0006	0.0007	-0.0001
2.0	-0.0005	0.0009	0.0019	-0.0001
5.0	-0.0009	0.0026	0.0082	-0.0002

*See Eqs. 3-7.

Table 4. Wind Data Used as Input for the Cincinnati Echoes Observed between 1200-1314 GMT

Level (mb)	Wind Velocity (deg - m/sec)	Lateral Shear (sec^{-1})
850	44.0 - 14.2	-2.78×10^{-5}
700	38.0 - 12.2	-1.86×10^{-5}
500	25.0 - 16.9	-1.39×10^{-5}

results for rainshowers instead of severe thunderstorms for which the model was originally developed. Figures 16 and 17 show the actual echo trajectory, the trajectory based on movement at the computed average wind velocity in the cloud layer, and six trajectories obtained from the model at different values of tangential velocity. Velocities from the model at 8-min intervals also are given. The drag coefficient was assumed to be 1.0. When cyclonic rotation was included in the model, results were worse than the trajectory based on the average wind velocity; however, when anticyclonic rotation was assumed, better trajectories were obtained. The trajectory computed using a tangential velocity of -2.0 m/sec produced the closest agreement with the observed track although its speed was too slow. Oscillations in the computed velocity also are evident in this example, and a comparison of the relative magnitudes of the forces considered shows that the lift force is still the most important. The trajectory based on a tangential velocity of -5.0 m/sec shows an abrupt curve which is associated with a significant increase and then a decrease in forward speed. This undesirable feature occurred often in cases of relatively small storms with large tangential velocities.

Instead of presenting many other examples of storm motion to illustrate various features and peculiarities of the model, these results will be presented qualitatively. Several hundred trajectories have been computed both by Veazey and as a part of this research to determine the behavior of the model under differing wind profiles, storm sizes, drag coefficients, etc. Trajectories were found to vary from straight lines, to curves and loops, but many of the tracks compared favorably to those observed in nature. Some important points based on work by Veazey and these investigators are as follows:

1. In some cases the speed of the storm was observed to increase well beyond the actual wind speed which was then associated with abrupt curves in the trajectory since the relative velocity is a factor in each of the force equations. The speed of the storm is very important in determining its trajectory. A method for including

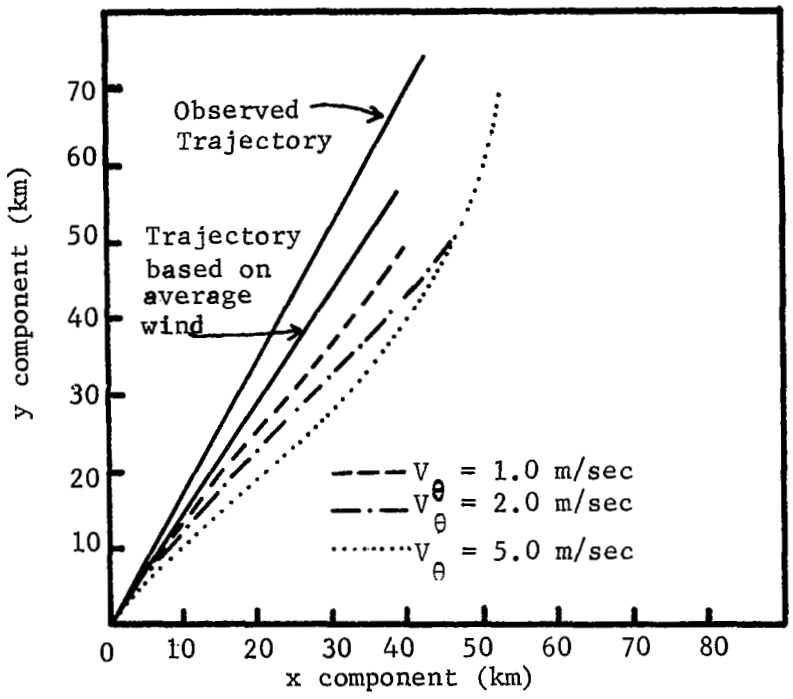

Computed Cloud Speeds (m/sec)

Time (min)	Assumed Tangential Velocity (m/sec)		
	V_θ =1.00	V_θ =2.00	V_θ =5.00
8	12.32	12.35	12.45
16	12.55	12.68	13.32
24	12.78	13.08	14.81
32	13.01	13.54	16.76
40	13.23	14.03	18.85
48	13.45	14.56	20.76
56	13.67	15.10	22.16
64	13.88	15.64	22.82
72	14.08	16.18	22.55
80	14.29	16.69	21.31

Fig. 16. Observed and computed cloud trajectories at rotation rates of 1.0, 2.0, and 5.0 m/sec for the Cincinnati echoes observed between 1200-1314 GMT. (The initial cloud velocity was assumed to be toward 38° at 12.2 m/sec, the echo diameter was 9.0 n mi, and the drag coefficient was 1.0. Computed cloud speeds are given to the right of the figure.)

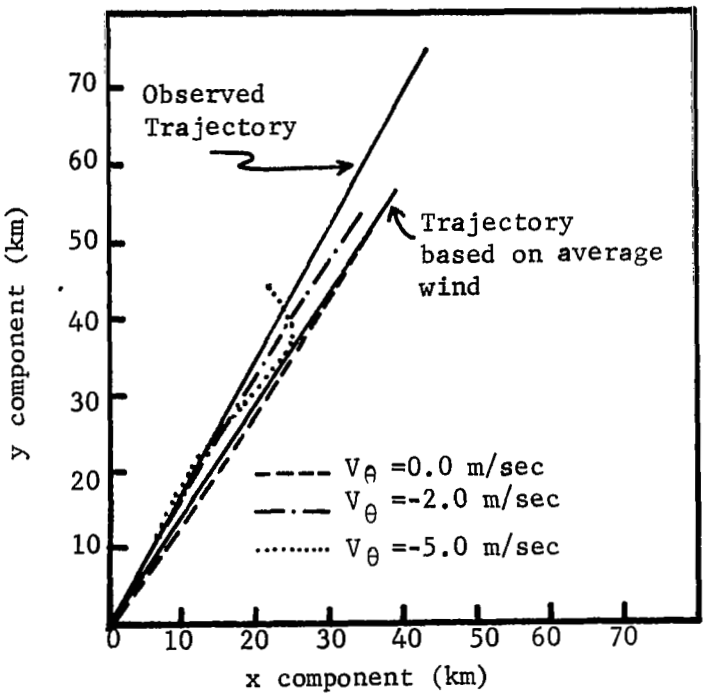

Computed Cloud Speeds (m/sec)

Time (min)	Assumed Tangential Velocity (m/sec)		
	V_θ =0.0	V_θ =-2.0	V_θ = -5.0
8	12.29	12.23	12.17
16	12.46	12.42	12.78
24	12.62	12.80	14.27
32	12.77	13.38	15.27
40	12.91	14.05	14.75
48	13.05	14.47	12.64
56	13.18	14.41	9.13
64	13.31	13.93	5.28
72	13.43	13.16	6.03
80	13.55	12.19	11.66

Fig. 17. Observed and computed cloud trajectories at rotation rates of 0.0, -2.0, and -5.0 m/sec for the Cincinnati echoes observed between 1200-1314 GMT. (The initial cloud velocity was assumed to be toward 38° at 12.2 m/sec, the echo diameter was 9.0 n mi, and the drag coefficient was 1.0. Computed cloud speeds are given to the right of the figure.)

the vertical transport of horizontal momentum in the model would probably reduce this problem. The assumption of an initial velocity other than the 700-mb value also may yield better results.

2. The environmental winds used as input for the model are likewise very important in determining the trajectory. Further research should be done to determine if different levels or a different weighting scheme produces better results.

3. Although the tangential velocities of specific clouds are not known, the value is important in determining numerical cloud trajectories. The lift force produced by cloud rotation acts to the right (left) of the instantaneous cloud velocity vector for cyclonically (anticyclonically) rotating storms that are moving slower than the wind. If a cloud is traveling faster than portions of the wind, the lift force is reversed. Nonrotating storms tend to move to the left of their instantaneous velocity vector. The magnitude of the lift force increases with increasing absolute values of tangential velocity, but only up to about $\pm$ 7 m/sec.

4. The drag coefficients for specific clouds are unknown. A smaller drag coefficient produces more deviation of the trajectory from the average wind for a given set of input conditions than a larger value since the drag force is parallel to relative velocity while the other forces are perpendicular to it. Larger drag coefficients tend to stabilize the motion of the cloud along the average wind direction.

5. The size of the cloud is also important in determining its stability. The lift force and drag force are smaller for a larger cloud than a smaller one if other factors remain constant.

6. Lateral shear generally has a small effect on cloud trajectories except in regions of pronounced shear. The force is directed normal and to the right of the relative wind vector for cyclonic shear and to the left for anticyclonic shear.

V. CONCLUDING REMARKS

This research has posed many unanswered questions about the observed motions of clouds relative to the ambient wind field and about the forces which lead to cloud movements. Although the assumptions used in developing the model described in this report are quite severe, the model shows promise in explaining observed cloud motions. As these assumptions are relaxed so that a more realistic model is obtained, results should improve considerably. Further research is currently being conducted to improve the model. By understanding the factors involved in cloud motions, better use can be made of the satellite pictures which are now obtained on a regular basis.

REFERENCES

Brooks, H. R., 1946: A summary of some thunderstorm observations. Bull. Amer. Meteor. Soc., 27, 557-563.

Byers, H. R., and R. R. Braham, Jr., 1949: The Thunderstorm, Washington, D.C., Government Printing Office, 287 pp.

Costen, R. C., 1972: Theory for the drift of severe local storms and hurricanes (abstract), EOS Trans. AGU, 53, 988.

Darkow, G. L., 1968: Deflecting forces on nonrotating convective systems due to environmental shear. Preprint of paper presented at the 6th Conference on Severe Local Storms, Chicago, Illinois, April 8-10, 1969, American Meteorological Society, Boston, Massachusetts, pp. 20-23 (unpublished manuscript.)

Fankhauser, J. C., 1964: On the motion and predictability of convective systems as related to the upper winds in a case of small turning of wind with height. Natl. Severe Storms Proj. Rep. No. 21, U.S. Wea. Bur., Washington, D.C., 36 pp.

Fujita, T., and H. Grandoso, 1968: Split of a thunderstorm into anticyclonic and cyclonic storms and their motion as determined from numerical model experiments. J. Atmos. Sci., 25, 416-439.

Hiser, H. W., and S. G. Bigler, 1953: Wind data from radar echoes. Urbana, Ill. State Water Survey, Meteor. Lab., Tech. Rep. No. 1, 18 pp.

Humphreys, W. J., 1940: Physics of the Air. McGraw-Hill Book Co., New York, New York, 359 pp.

Ligda, M. G. H., and W. A. Mayhew, 1954: On the relationship between the velocities of small precipitation areas and the geostrophic winds. J. Meteor., 11, 421-423.

Newton, C. W., and H. R. Newton, 1959: Dynamical interactions between large convective clouds and environment with vertical shear. J. Meteor., 16, 483-496.

Newton, C. W., and J. C. Fankhauser, 1964: On the movements of convective storms, with emphasis on size discrimination in relation to water-budget requirements. J. Appl. Meteor., 3, 651-668.

Newton, C. W., and S. Katz, 1958: Movement of large convective rainstorms in relation to winds aloft. Bull. Amer. Meteor. Soc., 39, 129-136.

REFERENCES (CONTINUED)

Ostergoard, P. B., 1948: Motion of storm cells as seen by radar. Cambridge, Mass. Inst. Tech. (Unpublished M.S. thesis).

Veazey, D. R., 1968: An investigation of the trajectories of rotating thunderstorms: a numerical experiment. College Station, Texas, Texas A&M University (Unpublished M.S. thesis).

NASA-Langley, 1975